Experimental Phase Diagram of a Binary Colloidal Hard-Sphere Mixture with a Large Size Ratio

A. Imhof and J. K. G. Dhont

Van't Hoff Laboratory for Physical and colloid Chemistry, Utrecht University, Padualaan 8, 3584 CH Utrecht, The Netherlands
(Received 2 May 1995)

We determined the phase diagram of a binary hard-sphere dispersion with size ratio 9.3. Phase separation into a fluid and a crystal of large spheres is observed. The fluid-solid binodal is determined by measurements of compositions of coexisting phases. The results agree qualitatively with recent theories, although the latter strongly overestimate the depletion activity of the smaller spheres. By fluorescent labeling we are able to measure the mobility of both particles separately. We found evidence for a new glassy phase in which only the small spheres are mobile.

In recent years there has been a considerable interest in the phase behavior of binary mixtures of hard spheres. This is mainly due to two results. The first is the prediction of a fluid-fluid instability in mixtures of hard spheres with a ratio a_L/a_S of large to small particle radii larger than ~ 5 [1]. The second is the observation of the formation of superlattice structures in binary hard-sphere colloids with size ratios of ~ 1.6 [2]. Colloidal dispersions are often used as model systems in studies of simple fluids because they provide accessible time and length scales and, in addition, particle interactions can easily be manipulated to closely approximate hard particles. The instability in a binary mixture with a large size ratio is due to an effective attraction between the large particles, called the depletion attraction [3], which is of a purely entropic nature. When two large particles approach each other, the smaller particles are expelled from the gap. The difference between the osmotic pressure in the gap and in the bulk induces the attraction. An important question is how this affects the phase behavior. The depletion effect is most clearly present in mixtures of colloidal hard spheres with polymer molecules. For binary colloids, in which also the small particles behave as hard spheres, the effect is often much less pronounced. So far only parts of the phase diagram have been obtained experimentally and they differ considerably from one system to the other [4–7]. A notable shortcoming of these previous investigations is the clear establishment of the nature of the coexisting phases. Two bulk disordered phases are always observed, but van Duijneveldt, Heinen, and Lekkerkerker [5] do not exclude the possibility that one of the phases crystallizes, and Kaplan *et al.* [6] observe some crystallization only on the walls of their containers, while Steiner , Meller, and Stavans [7] sometimes find a crystalline solid and sometimes an amorphous one. From the theoretical side it seems that the instability depends sensitively on the approximation used for the closure [1,8,9] or the activity of the small spheres [10,11].

In this Letter, we report the phase diagram of a new binary hard-sphere dispersion with size ratio $a_L/a_S = 9.3$. This system consists of charged silica spheres dispersed in dimethylformamide (DMF) in the high screening limit. We established for the first time, unambiguously, the nature of the coexisting phases: a colloidal fluid and a colloidal crystal formed by large spheres. In addition, by determining the compositions of the coexisting phases we located the fluid-solid binodal over a large part of the phase diagram, allowing a better test of recent theories. A special feature of our mixtures is that one of the species, either the larger or the smaller, is labeled with a fluorescent dye. This enables us to measure the mobility of both particles separately by measuring their long-time self-diffusion coefficients (D_s^L). In this way, evidence was found for a new unusual glass phase in which the large spheres are structurally arrested while the small spheres are still mobile.

We prepared colloidal silica particles of two different sizes, having hydrodynamic radii of 365 ± 5 and 39 ± 1 nm, measured with dynamic light scattering (DLS), and polydispersities of 0.03 and 0.12, respectively. Of both particles we prepared a separate batch in which the cores of the spheres were labeled with the fluorescent dye fluorescein isothiocyanate [12]. The solvent was DMF with $0.0100M$ LiCl. This corresponds to a Debye screening length of only 2.2 nm, making particle interactions essentially hard-sphere-like. From concentrated stock dispersions, mixtures were obtained in which either the small or the large particles are labeled. By varying the ratio of volume fractions of large and small spheres ϕ_L/ϕ_S, phase behavior was studied in the entire (ϕ_L, ϕ_S) plane, once with the small spheres labeled and once with the large spheres labeled. Mixtures were contained in tubes of diameter 5 or 10 mm and their phase behavior was observed over one or two days. In addition, small amounts were transferred to glass vials of thickness 0.2 or 0.4 mm and width 4 mm, which were monitored over a prolonged period of time. The large spheres sediment at a considerable rate (1 mm/h) in the more dilute samples. However, at higher volume fractions, where phase transitions occur, sedimentation is much slower and samples do not show significant sedimentation even after several days.

In the solvent used, the silica particles are stabilized against aggregation by a solvation layer of a few nanometer thickness on each particle surface. Such a layer presents a steeply repulsive force barrier and effectively screens attractive van der Waals forces, which become active only at very short particle separations [13]. The solvation layer also increases the specific or hydrodynamic particle volume. It can be detected most clearly around the small particles due to their relatively small size. For instance, dispersed in ethanol, their radius measured with DLS is 35 nm, 4 nm, smaller than the DLS radius in DMF. Also, the solvation layer showed up in a relatively large value of the intrinsic viscosity $[\eta]$. This quantity was determined by measuring the increase in the viscosity of the dispersion relative to the solvent η/η_0 over a range of dry silica volume fractions in the dilute limit: $[\eta] = \lim_{\phi \to 0}(\eta/\eta_0 - 1)/\phi$. For the small spheres we found $[\eta] = 3.8$ vs 3.0 for the large ones. The difference corresponds to a layer of 3 nm. The dry silica volume fractions, obtained by drying a weighted amount of stock dispersion, were converted to hydrodynamic volume fractions [14] by multiplying them by $[\eta]/2.5$, with 2.5 the Einstein value for the intrinsic viscosity.

Long-time self-diffusion coefficients were determined using fluorescence recovery after photobleaching (FRAP) [15]. The FRAP signal, denoted as $S(t)$, is proportional to the long-time self-intermediate scattering function, $\exp\{-D_s^L k^2 t\}$, with k the wave vector of the fringes, typically 10^5 to 10^6 m^{-1}. In this Letter we use FRAP only to characterize the mobility of both particles in the different phases. Extensive measurements of D_s^L will be presented elsewhere [16].

The nature of the different phases is indicated in Fig. 1(a). In the major part of the diagram the components form a homogeneous fluid mixture (F). Our phase diagram differs most notably from earlier investigations [4–7] in that we observed a phase separation into a fluid and a crystal formed by the large spheres. This occurred in a region ($F + C$) in the lower right-hand corner of the diagram, where $\phi_L > \phi_S$. Here crystals nucleated homogeneously throughout the samples, giving rise to visible Bragg reflections, and started moving towards the bottom of the vessel relatively quickly, forming a crystalline sediment. A FRAP signal of the large spheres, measured in the coexisting fluid, is shown in Fig. 2(a). It decays single exponentially to zero, as expected for a fluid. Our system did not show surface phase separation, due to depletion attraction between large particles and the wall [6]. At high volume fractions we identified two different glassy phases with FRAP. In the first we found that neither of the particle species was fully mobile, and we, therefore, indicate it by $G_L(G_S)$. In the other glass phase called $G_L(F_S)$, only the small particles were free to move. The $G_L(G_S)$ phase occurred when $\phi_S > \phi_L$. Here, the self-intermediate scattering function of neither the large nor the small particles showed a complete decay: Typical examples of FRAP curves are shown in Fig. 2(b). Notice the long time span of the experiments. Samples in this region were very viscous and the speckles in the scattering pattern of the large spheres were static, reflecting their immobility. The $G_L(F_S)$ phase was found in a region where ϕ_L exceeds ϕ_S. In this phase the FRAP curves of the large spheres again decayed only partly, and the scattering speckles were static. At the same time, however, FRAP curves of the small spheres invariably decayed to zero, although in a non-single-exponential way, Fig. 2(c). The small spheres thus have a complete relaxation. Samples in this region also appeared to be less viscous than
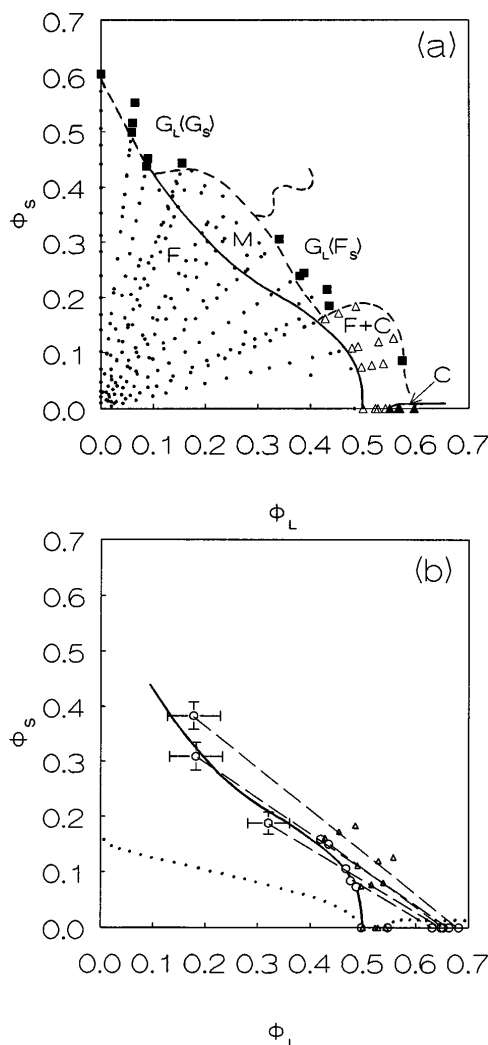

FIG. 1. (a) Phase diagram of the binary mixture. Dots represent homogeneous fluids, open triangles are samples separating into fluid and crystal, filled triangles are completely crystalline, filled squares are glassy samples. The solid line is the fluid-solid binodal from (b), dashed lines are glass transition lines. (b) Construction of the fluid-solid binodal (solid line). Triangles are compositions separating into fluid and crystal. Dashed lines are tie lines connecting coexisting compositions (circles). The dotted line is the theoretical prediction from Ref. [11].

those in the $G_L(G_S)$ phase. Possibly the small spheres are moving through a kind of porous medium formed by the static large spheres. The two modes seen in Fig. 2(c) are then explained by a fast intracavity diffusion and a much slower diffusion from one cavity to the next. We do not know the precise location of the line separating the two glassy states, if a Sharp transition exists at all. In the intermediate range the fluid region extends up to very high total volume fractions, where the samples become very hard to handle.

More information about the fluid-solid coexistence was obtained by constructing the fluid-solid binodal. The binodal consists of a freezing line with fluid phase compositions $(\phi_{f,L}, \phi_{f,S})$ and of a melting line with solid phase compositions $(\phi_{m,L}, \phi_{m,S})$. For the one-component large sphere system the freezing and melting volume fractions ϕ_f and ϕ_m were determined in the usual way [17]: The fraction of the system occupied by the equilibrium crystal phase f_{cryst} is found from the height of the sediment after the crystallites have settled. Effects of particle sedimentation and sediment compaction are ruled out by monitoring the subsequent linear growth of the sediment and extrapolating this to zero time. f_{cryst} increases linearly with the overall volume fraction and extrapolates to zero

at ϕ_f and to unity at ϕ_m. We found $\phi_f = 0.497 \pm 0.004$ and $\phi_m = 0.547 \pm 0.004$, close to the well-known hard-sphere values of 0.494 and 0.545 [18].

For binary mixtures, points on the freezing and melting lines must be found by determining the composition of one of the phases. Together with f_{cryst} the composition of the coexisting phase can then be found with the lever rule. The volume fraction of small spheres in the crystal can be taken to zero, since even if the octahedral and tetrahedral sites were completely filled with small spheres, their volume fraction does not exceed 0.01. We determined the volume fraction of large spheres in the crystal from measurements of the Bragg diffraction angle 2θ at the first diffraction maximum. To this end a sample cuvette of 0.2 mm path length was placed in a cylindrical bath filled with DMF/0.01M LiCl to avoid refraction at the interface and illuminated by a 633 nm laser beam. Care was taken to measure the Bragg angle while the crystallites were still sedimenting, since otherwise the lattice spacing is reduced by gravitational compaction. Ascribing the diffraction maximum to a fcc (111) reflection the lattice constant b follows from $(2nb\sin\theta/\lambda)^2 = 3$, where n is the solvent refractive index and λ the wavelength *in vacuo*. The volume fraction of large spheres in the crystal is then $\phi_{m,L} = 16\pi a_L^3/3b^3$. Although the crystal structure was not determined, it is noted that hexagonal close packing leads to exactly the same $\phi_{m,L}$, whereas bcc yields an unrealistically small value. The uncertainty of 1.4% in a_L leads to errors of 4% in $\phi_{m,L}$. To avoid making such a large error we calculated $\phi_{m,L}$ by comparing b to the value found in a monodisperse system (1154 nm), so that $\phi_{m,L} = 0.547[(1154 \text{ nm})/b]^3$. The resulting error in $\phi_{m,L}$ is estimated to be 1%. Compositions of coexisting phases thus found are given in Table I. It is seen that addition of the smallest amount of small spheres already leads to a large decrease in lattice constant. This is caused by the osmotic pressure exerted on the crystal by the abundance of small particles in the fluid. This pressure is exactly the effective entropic attraction that drives the large spheres together and which causes the freezing transition to occur at smaller ϕ_L as ϕ_S is increased.

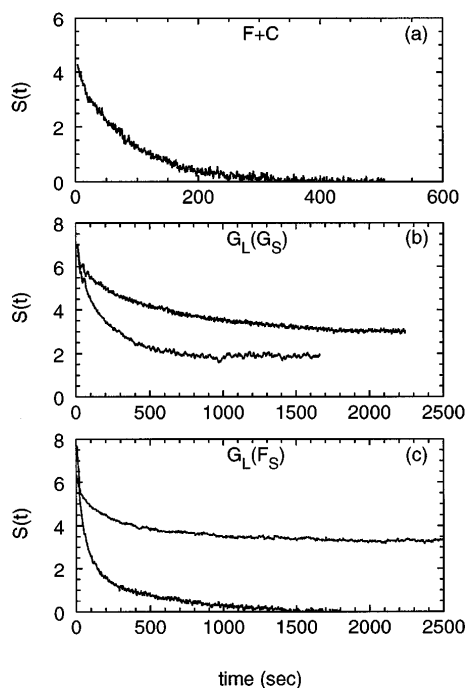In Fig. 1(b) the fluid-solid binodal is shown, with coexisting phases connected by tie lines. Additional

FIG. 2. (a) FRAP signal $S(t)$ of the large spheres measured in the fluid coexisting with the crystal ($\phi_L = 0.505$, $\phi_S = 0.910$, $k = 780\,240$ m^{-1}). (b) FRAP signals in the $G_L(G_S)$ phase; large spheres (lower curve, $\phi_L = 0.0592$, $\phi_S = 0.499$, $k = 463\,320$ m^{-1}), small spheres (upper curve, $\phi_L = 0.0609$, $\phi_S = 0.516$, $k = 206\,060$ m^{-1}). (c) FRAP signals in the $G_L(F_S)$ phase; large spheres (upper curve, $\phi_L = 0.435$, $\phi_S = 0.184$, $k = 451\,660$ m^{-1}), small spheres (lower curve, $\phi_L = 0.379$, $\phi_S = 0.239$, $k = 203\,700$ m^{-1}).

TABLE I. Compositions of coexisting fluid and crystalline phases.

Overall		Crystal Phase		Fluid Phase			
ϕ_L	ϕ_S	$\phi_{m,L}$	$\phi_{m,S}$	$\phi_{f,L}$	$\phi_{f,S}$	f_{cryst}	b (nm)
0.529	0	0.547	0	0.497	0	0.65	1154
0.539	0.081	0.664	0	0.182	0.309	0.74	1082
0.517	0.077	0.653	0	0.321	0.188	0.59	1088
0.477	0.074	0.632	0	0.477	0.084	0.12	1100
0.490	0.111	0.649	0	0.435	0.150	0.26	1090
0.428	0.162	0.682	0	0.178	0.383	0.55	1072

points on the freezing line were found by diluting mixtures at constant ϕ_L/ϕ_S until crystallization was no longer observed. Included in the figure is the theoretical binodal from [11]. Since we do not observe a fluid-fluid separation, the phase diagram agrees with recent predictions that a fluid-fluid spinodal is metastable with respect to the fluid-solid [10,11]. The shape of the $F + C$ coexistence region also agrees qualitatively with these theories. However, the latter strongly overestimate the depletion activity of the small spheres. In our system phase separation is found at larger σ_S than in Refs. [5–7]. The binodals found in those investigations also differ considerably from each other. Since in each case different model particles were used, it seems that the binodal depends sensitively on small deviations from true hard-sphere behavior.

Figure 1(a) includes the fluid-solid binodal from Fig. 1(b). Although the binodal extends over the full width of the phase diagram, actual crystallization is observed only in a limited region ($F + C$) where $\phi_L > \phi_S$. This indicates that the homogeneous fluid phases found above part of the binodal are metastable with respect to the fluid-solid binodal (region M). In such systems D_s^L of a large sphere was more than 50 times smaller than its value at infinite dilution [16]. It is, therefore, not surprising that crystallization rates are extremely small. Indeed, the time needed for crystallites to become visible increased from ~15 min for monodisperse systems, through several hours for the $\phi_L > \phi_S = 6.696$ mixture, to almost two days for $\phi_L/\phi_S = 2.650$. In the part labeled with M no crystallization was observed, even over a period of several days.

In conclusion, we determined the phase diagram of a new binary hard-sphere model dispersion. We established a phase separation into a fluid and a crystal phase, which is different from earlier observations. Just as theoretical predictions are very sensitive to the approximations used, so are experimental phase lines probably extremely sensitive to small deviations from true hard-sphere behavior of the model particles used. Based on the absence of fluid-fluid phase separation and on the location of the fluid-crystal binodal we conclude that current theories qualitatively agree with our observations, but that they strongly overestimate the depletion activity of the small particles. In addition, we found two different glass states.

[1] T. Biben and J. P. Hansen, Phys. Rev. Lett. **66**, 2215 (1991).

[2] S. Hachisu and S. Yoshimura, Nature (London) **283**, 188 (1980); P. Bartlett, R. H. Ottewill, and P. N. Pusey, J. Chem. Phys. **93**, 1299 (1990); Phys. Rev. Lett. **68**, 3801 (1992).

[3] S. Asakura and F. Oosawa, J. Polym. Sci. **32**, 183 (1958); A. Vrij, Pure Appl. Chem. **48**, 471 (1976).

[4] S. Sanyal, N. Easwar, S. Ramaswamy, and A. K. Sood, Europhys. Lett. **18**, 107 (1992).

[5] J. S. van Duijneveldt, A. W. Heinen, and H. N. W. Lekkerkerker, Europhys. Lett. **21**, 369 (1993).

[6] P. D. Kaplan, J. L. Rouke, A. G. Yodh, and D. J. Pine, Phys. Rev. Lett. **72**, 582 (1994).

[7] U. Steiner, A. Meller, and J. Stavans, Phys. Rev. Lett. **74**, 4750 (1995).

[8] J. J. Lebowitz and J. S. Rowlinson, J. Chem. Phys. **41**, 133 (1964).

[9] Y. Rosenfeld, Phys. Rev. Lett. **72**, 3831 (1994).

[10] H. N. W. Lekkerkerker and A. Stroobants, Physica (Amsterdam) **195A**, 387 (1993).

[11] W. C. K. Poon and P. B. Warren, Europhys. Lett. **28**, 513 (1994).

[12] A. van Blaaderen and A. Vrij, Langmuir **8**, 2921 (1992).

[13] G. Peschel *et al.,* Colloid Polym. Sci. **260**, 444 (1982); A. Grabbe and R. G. Horn, J. Colloid Interface Sci. **157**, 375 (1993).

[14] C. G. de Kruif, E. M. F. van Iersel, and W. B. Russel, J. Chem. Phys. **83**, 4717 (1985).

[15] A. Imhof, A. van Blaaderen, G. Maret, J. Mellema, and J. K. G. Dhont, J. Chem. Phys. **100**, 2170 (1994).

[16] A. Imhof and J. K. G. Dhont (to be published).

[17] S. E. Paulin and B. J. Ackerson, Phys. Rev. Lett. **64**, 2663 (1990).

[18] W. G. Hoover and F. H. Ree, J. Chem. Phys. **49**, 3609 (1968).